

RSC Advances



This is an *Accepted Manuscript*, which has been through the Royal Society of Chemistry peer review process and has been accepted for publication.

Accepted Manuscripts are published online shortly after acceptance, before technical editing, formatting and proof reading. Using this free service, authors can make their results available to the community, in citable form, before we publish the edited article. This *Accepted Manuscript* will be replaced by the edited, formatted and paginated article as soon as this is available.

You can find more information about *Accepted Manuscripts* in the [Information for Authors](#).

Please note that technical editing may introduce minor changes to the text and/or graphics, which may alter content. The journal's standard [Terms & Conditions](#) and the [Ethical guidelines](#) still apply. In no event shall the Royal Society of Chemistry be held responsible for any errors or omissions in this *Accepted Manuscript* or any consequences arising from the use of any information it contains.



Mono- and binuclear palladacycles via regioselective C–H bond activation: syntheses, mechanistic insights and catalytic activity in direct arylation of azoles†

Received 00th January 20xx,
Accepted 00th January 20xx

DOI: 10.1039/x0xx00000x

www.rsc.org/

Dilip K. Pandey,^a Shrikant M. Khake,^a Rajesh G. Gonnade^b and Benudhar Punji^{*a}

Regioselective C–H bond palladation of the hybrid pincer-type ligands, 3-R₂PO-C₆H₄-1-CH₂NⁱPr₂ [^{R2}POCN^{iPr2}-H; R = Ph (**1a**), R = Et₂N (**1b**)] has been described to accomplish mono- and binuclear palladacycles. The reactions of the ligands ^{R2}POCN^{iPr2}-H (**1a**, **1b**) with Pd(COD)Cl₂ in the presence of K₃PO₄ afforded the mononuclear pincer complexes {κ^P, κ^C, κ^N-2-(R₂PO)-C₆H₃-6-(CH₂NⁱPr₂)}PdCl (^{R2}POCN^{iPr2})PdCl [R = Ph (**2a**), R = Et₂N (**2b**)], whereas the similar reactions in the presence of Et₃N produced the chloro-bridged binuclear palladacycles [{κ^P, κ^C-2-(R₂PO)-C₆H₃-4-(CH₂NⁱPr₂)}(μ-Cl)Pd]₂ (R = Ph (**4a**), R = Et₂N (**4b**)) via the regioselective ligands C(2)-H and C(4)-H bond activation, respectively. Similarly, the reaction of a previously reported ligand ^{iPr2}POCN^{iPr2}-H (**1c**) with Pd(COD)Cl₂ in the presence of Et₃N affords chloro-bridged binuclear complex [{κ^P, κ^C-2-(ⁱPr₂PO)-C₆H₃-4-(CH₂NⁱPr₂)}(μ-Cl)Pd]₂ (**4c**) via the regioselective C(4)-H bond palladation. On contrary, using Pd(OAc)₂ instead of Pd(COD)Cl₂ in the palladation reaction of **1a**, in presence or absence of base, leads to the exclusive formation of acetate-bridged binuclear palladacycle [{κ^P, κ^C-2-(Ph₂PO)-C₆H₃-4-(CH₂NⁱPr₂)}(μ-OAc)Pd]₂ (**5a**). Mechanistic detail for this regioselective C–H bond activation to achieve mono- and binuclear palladacycles has been demonstrated, which highlights that the coordinating ability of external base, steric between coordinated base and N-arm of POCN ligand as well as the electrophilicity of the palladium center are crucial to the regioselective palladation. The palladium complex **4c** was shown to be the active catalyst for the direct arylation of azoles with aryl iodides under mild reaction conditions.

Introduction

Palladacycles containing C-anionic four-electron donor (CE) or six-electron donor (ECE) ligand (E = donor group) have many attractive structural features.¹ The stable chelating structure and strong metal-carbon σ-bond provides them with high air and thermal stability, whereas the appropriate tuning of the substituents on donor-atom furnishes distinct sterics and electronics around the palladium; which make the palladacycles extraordinary catalysts for various important organic transformations.^{2,3} Though, each of these palladacycles has its own unique chemistry, the ECE-pincer (NCN,⁴ PCP,⁵ SCS,⁶ etc.) palladium system has attracted considerable interest, as it benefits from the advantage of terdentate coordination and hence, the well-protected palladium center.

Recently, the unsymmetrical ECE'-pincer palladium system having two different donor arms, typically one soft P-donor and one hard N- or O-donor, such as PCN,⁷ POCN,⁸ and PCO⁹ has given particular attention, as such system renders complementary properties of both the hard/soft donor as well as that of the distinct electron-donor/acceptor ability. In addition, the hemilabile palladacycles could provide suitable sterics, electronics, and coordination demands needed on the different steps of a catalytic reaction, and might produce the interesting structural motifs on stoichiometric reactions.

^a Organometallic Synthesis and Catalysis Group, Chemical Engineering Division, CSIR–National Chemical Laboratory (CSIR–NCL), Dr. Homi Bhabha Road, Pune – 411 008, Maharashtra, INDIA. Phone: + 91-20-2590 2733, Fax: + 91-20-2590 2621, E-mail: b.punji@ncl.res.in.

^b Centre for Material Characterization, CSIR–National Chemical Laboratory (CSIR–NCL), Dr. Homi Bhabha Road, Pune – 411 008, Maharashtra, INDIA.

†Electronic Supplementary Information (ESI) available: Crystallographic information files (CIF). NMR and mass spectra of ligands and complexes, crystal structure data of complexes **2a**, **2b**, **3a**, **3b** and **5a**. CCDC-1063772 (**2a**), CCDC-1063769 (**2b**), CCDC-1063773 (**3a**), CCDC-1063770 (**3b**) and CCDC-1063774 (**5a**). For ESI and crystallographic data in CIF or other electronic format see DOI: 10.1039/x0xx00000x

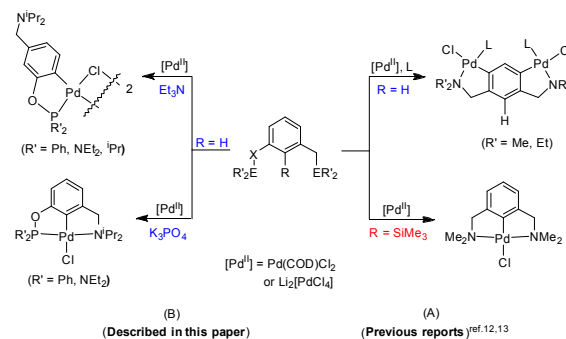


Chart 1 Representation of site-selective palladation to obtain aryl-based CE- or ECE-palladacycles: (A) by introduction of an activation group (-SiMe₃), (B) by regioselective C–H bond activation.

ARTICLE

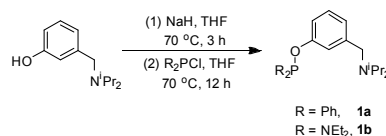
RSC Advances

Considering the broad applicability of the palladacycles, the efficient and regioselective synthesis of the hemilabile ECE'-based palladacycles (both CE- and ECE'-type) by C-H bond activation is indispensable. In general, the syntheses of the arene-based ECE pincer-palladium complexes, containing 1,3-donor group substituents, are executed by the direct cyclopalladation at C-2 position of the arene ligands; which usually promoted by the coordination of the donor groups on ligand prior to the intramolecular C(2)-H bond activation.^{10,11} However, in some of the pincer-type ligands, the cyclopalladation of C-2 does not occur and instead the C-4/C-6 palladation takes place to generate CE-type palladacycles (Chart 1A, top).¹² In order to obtain the selective ECE-pincer palladacycles, in such cases, the site selectivity of the palladation is inverted by the introduction of an activating group (-SiMe₃) at C-2 position (Chart 1A, bottom).^{12b,13} Surprisingly, the synthesis of both the CE- and ECE/ECE'-palladacycles from a single ECE/ECE' pincer-type ligand *via* the selective C-H bond palladation has not been precedented in the literature. We assumed that in an unsymmetrical pincer-type ligand POCN-H, as it contain two different donor groups with the distinct donating ability, the reactivity of the ligand towards palladium could be tuned to allow only P- or both N- and P-coordination, which would be followed by the regioselective C-H bond palladation to generate both type of palladacycles (CE- and ECE'-type), without being the introduction of an activating group (-SiMe₃). With this in mind and as a part of our research interest on the development of unsymmetrical pincer-systems,¹⁴ herein, we report the syntheses of two unsymmetrical POCN pincer-type ligands, and their regioselective C-H bond palladation to accomplish both the "PC"-chelate binuclear [κ^P, κ^C -PC-PdCl]₂ (CE-type) and "POCN"-coordinated mononuclear ($\kappa^P, \kappa^C, \kappa^N$ -POCN)PdCl (ECE'-type) palladacycles (Chart 1B). Furthermore, the influence of base on the regioselective C-H bond palladation is demonstrated, and the mechanistic aspect of the same has been elucidated. All the palladacycles were screened as a catalyst precursor for the direct C-H bond arylation of azoles with aryl iodides and some of them were efficiently employed in the synthesis of 2-arylated azoles.

Results and discussion

Synthesis of ligands

The R²POCN^{iPr₂}-H [3-R₂PO-C₆H₄-1-CH₂N^{iPr₂}] (R = Ph, **1a**; R = Et₂N, **1b**) pincer ligands were synthesized following the procedure similar to the synthesis of analogous compounds,¹⁴ which has been recently developed in our group. Hence, the treatment of 3-((diisopropylamino)methyl)phenol with NaH, followed by the reaction with relevant chlorophosphine produced the hybrid ligands **1a** and **1b** in good yields (Scheme 1). The ³¹P{¹H} NMR spectra of **1a** and **1b** showed single resonances at 109.7 and 131.8 ppm, respectively; which were comparable with the ³¹P NMR data of the similar compounds *i.e.* Ph⁴POCOP-H^{3c} (δ_p 114.0 ppm) and 4-Me-C₆H₄-OP(NEt₂)₂¹⁵ (δ_p 133.0 ppm). In the ¹H NMR spectra of both the compounds,

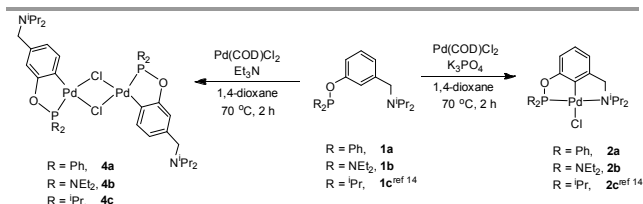


Scheme 1 Synthesis of POCN-H ligands.

the -CH₂ protons on -CH₂N^{iPr₂} group appeared around 3.60 ppm as singlets. Further, the assigned molecular structures of the compounds **1a** and **1b** are consistent with the observed ¹H and ¹³C NMR data. These compounds were used for the metallation reactions without further purification.

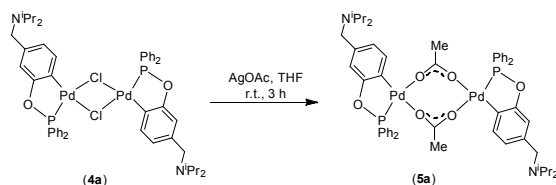
Synthesis of palladacycle complexes

Following our previous protocol for the synthesis of POCN pincer-palladium complexes,¹⁴ the reactions of **1a** and **1b** with Pd(COD)Cl₂ in the presence of inorganic base K₃PO₄ in 1,4-dioxane produced the pincer-ligated complexes { $\kappa^P, \kappa^C, \kappa^N$ -2-(R₂PO)-C₆H₃-6-(CH₂N^{iPr₂})}PdCl [(^{R₂}POCN^{iPr₂})PdCl]; R = Ph (**2a**) and R = Et₂N (**2b**) (Scheme 2). The ³¹P{¹H} NMR spectra of **2a** and **2b** displayed singlets at 150.0 and 142.3 ppm, respectively. In the ¹H NMR spectrum of **2a**, the -CH₃ protons (12H) of isopropyl groups appeared as two set of doublets in contrast to a single set of doublet observed for the same (12H) in **1a**, which could be due to the magnetic non-equivalency of -CH₃ protons, generated upon the coordination of N-arm of the ligand to the palladium center. The two -CH protons on the isopropyl groups appeared as an octet, which might be due to the partial overlapping of the two septets for each -CH of the -N{CH(CH₃)₂}₂ group. Similarly, the -CH₃ protons on isopropyl groups of the **2b** resonate differently and appeared as two distinct doublets. The appearance of two set of doublets for the -CH₃ protons on -N{CH(CH₃)₂}₂ groups in the complexes **2a** and **2b**, in contrast to single set of doublet in the ligands **1a** and **1b**, could be considered as an indication for the nitrogen-arm coordination to the palladium center. Further, the peak of -CH₂ protons on the -CH₂N^{iPr₂} group of **2a** and **2b** deshielded (~ 0.4 ppm) compared to the respective ligands, and appeared around 4.0 ppm as singlets. The POCN-pincer palladium complexes **2a** and **2b** were further characterized by ¹³C NMR, MALDI-TOF measurements and elemental analyses. The proton and carbon peaks chemical shift in both the complexes were fully assigned by the 2D NMR studies, after establishing the atom connectivity and spatial relationship. The molecular structures of **2a** and **2b** were also confirmed by the single crystal X-ray diffraction studies.

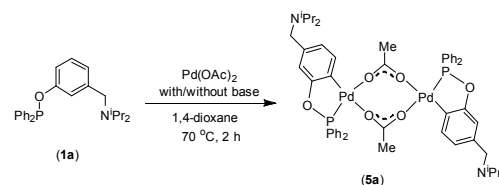


Scheme 2 Synthesis of palladacycle complexes.

To our surprise, the reactions of **1a**, **1b** and **1c**¹⁴ with Pd(COD)Cl₂ in the presence of Et₃N as base in 1,4-dioxane produced the binuclear *ortho*-palladated complexes $[\{\kappa^P, \kappa^C\text{-}2\text{-}(\text{R}_2\text{PO})\text{-C}_6\text{H}_3\text{-}4\text{-}(\text{CH}_2\text{N}^i\text{Pr}_2)\}\{\mu\text{-Cl}\}\text{Pd}]_2$ $\{\text{R} = \text{Ph}$ (**4a**), Et₂N (**4b**), ⁱPr (**4c**) $\}$, with the chloride as a bridging ligand between the two palladium centers (Scheme 2). In the binuclear complexes, each palladium center is coordinated by the P-atom, and the C-atom that is *ortho* to –OPR₂ and *para* to –CH₂NⁱPr₂ group. Unlike the pincer-ligated complexes **2a**, **2b**, and **2c**,¹⁴ the N-arm of the ligand in binuclear complexes (**4a**, **4b** and **4c**) does not involved in the coordination to palladium center. It should be noted that the triethylamine (Et₃N) is commonly used as a base for the synthesis of pincer-ligated palladium complexes; however, in the current ligand systems the formation of non-pincer *ortho*-palladated binuclear complexes were observed in the presence of Et₃N, even though the ligands are of pincer-type. To our knowledge, this represents the first example of a base-assisted site selective C–H bond palladation to accomplish both the bidentate-coordinated palladacycles and terdentate-coordinated pincer palladium complexes from the pincer-type ligands. Similar site selective palladation has previously been known only by the introduction of an activating group (i.e. –SiMe₃).^{12,13,16} The ³¹P NMR spectrum of **4a** displayed two singlets at 152.9 and 152.2 ppm in 1.5 : 1 ratio. The two different peaks could be due to the existence of *cis* and *trans* isomers for the complex **4a** in solution.¹⁷ Though, the ³¹P NMR data of **4a** is suggestive of two isomers, the ¹H NMR spectrum displayed a single set of peaks. The –CH₃ protons on the –NⁱPr₂ group showed only one broad singlet at 1.00 ppm, suggesting the N-arm of the ligand is not involved in the coordination to Pd-center. Further, the peak at 3.55 ppm for the –CH₂ protons on –CH₂NⁱPr₂ group is indicative of a non-coordinating N-arm. The MALDI-TOF spectrum of **4a** displayed the molecular ion peak at 1063.3624, which is consistency with the existence of a binuclear complex. Similar to the complex **4a**, the ³¹P NMR spectrum of binuclear complex **4b** displayed two singlets at 137.7 (76%) and 137.9 (24%) ppm for the two different isomers. The ¹H NMR spectrum showed a single set of peaks and the splitting pattern of the proton peaks resemble to that observed for a non-coordinating –CH₂NⁱPr₂ group. The ³¹P NMR spectrum of the complex **4c** showed two singlets at 200.0 and 199.0 ppm for the presumed two isomers in 1.9:1 ratio. The ¹H NMR spectrum exhibited a single set of peaks with the distinctive of non-coordinated –CH₂NⁱPr₂ and coordinated –OPⁱPr₂ groups. The MALDI-TOF measurement displayed the peaks at 1043.4058 (M+H)⁺ and 927.3241 (M+H)⁺ for the binuclear complexes **4b** and **4c**, respectively.



Scheme 3 Synthesis of acetate-bridged binuclear palladium complex **5a**.



Scheme 4 Palladation of **1a** with Pd(OAc)₂.

To synthesize the derivative of a binuclear palladacycle, the complex **4a** was treated with AgOAc which generated the acetate-bridged binuclear complex $[\{\kappa^P, \kappa^C\text{-}2\text{-}(\text{Ph}_2\text{PO})\text{-C}_6\text{H}_3\text{-}4\text{-}(\text{CH}_2\text{N}^i\text{Pr}_2)\}\{\mu\text{-OAc}\}\text{Pd}]_2$ (**5a**) (Scheme 3). The ³¹P NMR spectrum of **5a** displayed a singlet at 151.0 ppm, which is slightly shielded than that observed for the chloro-bridged complex **4a**. Unlike the complex **4a**, the acetate-bridged binuclear complex **5a** exists as a single isomer in solution as indicated from the ³¹P NMR data. The ¹H NMR data of **5a** resembled with that of the **4a**, except that the –CH₃ protons of bridged-acetate show a singlet at 2.17 ppm. Further, the ¹³C NMR data and elemental analysis of **5a** is in good agreement with the assigned structure. The molecular structure of complex **5a** was further confirmed by X-ray diffraction study.

On a different note, the C–H bond palladation of the R²POCNⁱPr₂–H ligand was explored with other palladium precursor like Pd(OAc)₂. Surprisingly, the reaction of Ph²POCNⁱPr₂–H (**1a**) with Pd(OAc)₂ in the presence of K₃PO₄ produced the *ortho*-palladated binuclear palladacycle **5a**, rather than the presumed mononuclear pincer complex (Scheme 4). Further, the same reaction in the presence of Et₃N or even in the absence of a base afforded the binuclear complex **5a**. These results indicated that the base has no influence on the regioselective palladation of the ligand **1a** while Pd(OAc)₂ is used as a palladium source. This distinct reactivity of **1a** with Pd(OAc)₂ than with the Pd(COD)Cl₂ towards the regioselective palladation can be attributable to the electrophilic character of Pd(OAc)₂. The high electrophilicity of Pd(OAc)₂ could accelerate the electrophilic attack of the Pd-center on arene ring of the POCN–H ligand after the P-arm coordination, leading to palladacycle **5a**, rather than allowing both the P- and N-arm coordination and C_{*ipso*}–H bond palladation.

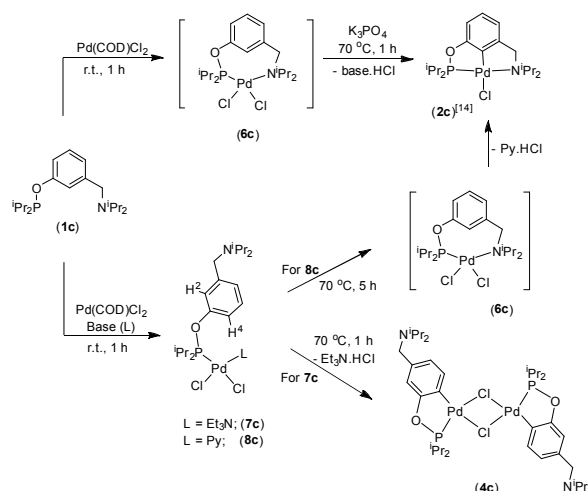
Mechanistic aspects of regioselective palladation

The reactions of the ligands **1a-1c** with Pd(COD)Cl₂ in the presence of K₃PO₄ produce the pincer complexes **2a-2c** by the arene C(2)–H bond activation of the 1,3-donor group substituted ligands, whereas the similar reactions in the presence of triethylamine exclusively furnished the non-pincer *ortho*-palladated binuclear palladacycles **4a-4c** through the C(4)–H bond activation, leaving the N-arm non-coordinated. In view of the synthetic aspect of the palladacycle complexes, this regioselective C–H bond palladation is unique as a base could decides the outcome of the products formation, i.e. mononuclear pincer complex or binuclear non-pincer complex. This distinct reactivity of the hybrid ligands **1a-1c** motivated us to investigate the mechanistic aspects of the regioselective

ARTICLE

RSC Advances

palladation reaction. We have chosen **1c** as a model ligand to study its reactivity with Pd(COD)Cl₂ under controlled reaction conditions, and the progress of the reaction was monitored by the ³¹P NMR analysis. Initially, the ligand **1c** was treated with Pd(COD)Cl₂ in 1,4-dioxane in the absence of base at room temperature (Scheme 5). After 1 h, the ³¹P NMR spectrum of the crude reaction mixture displayed two singlets at 198.2 and 141.6 ppm. The peak at 198.2 ppm corresponds to the pincer-ligated complex **2c**.¹⁴ The phosphorous peak at δ_p 141.6 ppm was tentatively assigned for the intermediate complex **6c**, as the HRMS (ESI) measurement of the crude reaction mixture showed a mass peak at m/z 522.0696 (m/z calcd for [6c+Na]⁺ = 522.0682). Several attempts to isolate the pure product of **6c** were unsuccessful, as the reaction was always resulted with the mixture of both **2c** and **6c**. However, upon addition of K₃PO₄ to the reaction mixture, a clean conversion of the mixture to the compound **2c** was occurred at elevated temperature. This suggests that the chelate complex **6c** is most likely an active intermediate for the formation of pincer-complex **2c** in the presence of K₃PO₄. Similar chelate complex intermediate [κ^S, κ^S -(MeS-CH₂)₂-C₆H₄-PdCl₂] for the synthesis of symmetrical pincer complex [$\kappa^S, \kappa^C, \kappa^S$ -(MeS-CH₂)₂-C₆H₃-PdCl] has previously been described.^{6a} Further, to understand the effect of Et₃N on the palladation reaction, the ligand **1c** was treated with Pd(COD)Cl₂ in the presence of Et₃N (1.2 equiv) in 1,4-dioxane at room temperature and the progress of the reaction was monitored by ³¹P NMR analysis. After stirring the reaction mixture for 1 h, the ligand peak at δ_p 148.8 ppm completely disappeared and the formation of a new peak at δ_p 143.6 ppm was observed, with the minor formation of complex **4c** (δ_p 200.6 ppm). The peak at δ_p 143.6 ppm was tentatively assigned to the intermediate palladium complex **7c** (Scheme 5), as the phosphorous ligands environment in **6c** and **7c** are almost similar and the ³¹P NMR chemical shifts for both of them were around in the same region (δ_p 141.6 and 143.6 ppm). An attempt to the isolation and characterization of the presumed intermediate complex **7c** was unsuccessful, as the probable hemilabile species **7c** was completely transformed into the thermodynamically stable product **4c** during the work-up process. Assuming that the hemilabile nature of Et₃N ligand might play a role in the instability of **7c**, the ligand **1c** was treated with Pd(COD)Cl₂ in the presence of pyridine (1.2 equiv) in 1,4-dioxane. After the reaction mixture was stirred at room temperature for 1 h, the ³¹P NMR measurement of the reaction mixture displayed a peak at 144.9 ppm with the complete disappearance of the peak correspond to **1c**. The ³¹P NMR peak at 144.9 ppm was assigned to the complex **8c**. The compound **8c** was isolated and fully characterized by the major spectroscopic techniques. In ¹H NMR spectrum of **8c**, the downfield shift (ca. 0.6 ppm) of the C(2)-H and C(6)-H protons on pyridine moiety suggests the pyridine ligand coordination to the palladium center. Further, the HRMS (ESI) analysis of the complex **8c** confirmed the assigned molecular structure. Since the ³¹P NMR chemical shifts of the three intermediate complexes (**6c**, **7c** and **8c**) were around in the same region, we



Scheme 5 Proposed pathway for the formation of “PC”- and “POCN”-palladacycles.

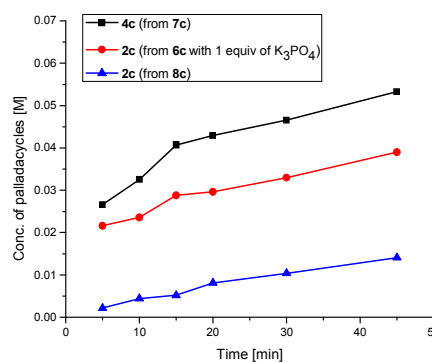


Fig. 1 Reaction profile for the C–H bond palladation of **6c**, **7c** and **8c** at 70 °C.

assumed that the assigned structures for these intermediates are appropriate. To our surprise, when the complex **8c** was heated in 1,4-dioxane at 70 °C for 5 h, the formation of pincer complex **2c** was observed, instead of the expected *ortho*-palladacycle complex **4c**. The formation of the pincer complex **2c** from the intermediate **8c** can be attributable to the easy displacement of the less bulky pyridine ligand by the –CH₂NⁱPr₂ ligand arm leading to the formation of an intermediate species **6c**, which is followed by the C(2)–H bond palladation. However, in the case of intermediate **7c**, the steric hindrance between –CH₂NⁱPr₂ group and coordinated Et₃N ligand might keep the –CH₂NⁱPr₂ unit away from the palladium center and allow the C(4)–H bond activation to produce the complex **4c**.

In order to gain more insight into the influence of base during the course of C–H bond palladation reaction, the kinetics of the electrophilic palladation step in the formation of **2c** and **4c** from the **6c** (or **8c**) and **7c**, respectively, were determined. All the kinetic experiments were performed after being the in situ generation of the intermediate species **6c**, **7c** and **8c** (For details, see SI). Initially the rates for the formation of products **2c** and **4c** were determined by employing one equiv of each base K₃PO₄, Et₃N and pyridine using the initial

rate approximation. The reaction profile for the C–H bond palladation on **6c**, **7c** and **8c** over a period of 45 min is shown in Fig 1. The rate for the formation of **4c** from the **7c** ($1.14 \times 10^{-3} \text{ Mmin}^{-1}$) is determined to be approximately four times faster than the formation of **2c** from **8c** ($0.296 \times 10^{-3} \text{ Mmin}^{-1}$). This indicates that the dissociation of coordinated Et_3N and C–H bond palladation in **7c** is much faster than the dissociation of pyridine and palladation in the complex **8c**.

Furthermore, the order of palladation reaction in each base was determined individually at 70°C in 1,4-dioxane with varying concentration of base using the initial rate approximation. The plot was drawn between $\log(\text{rate})$ vs. $\log(\text{conc. base})$, wherein the slope of the plot indicates the order of palladation reaction with the particular base. Figure S1 shows the rate of the palladation reaction is almost same for the various concentration of the K_3PO_4 , suggesting the reaction is zeroth-order in the concentration of K_3PO_4 . However, the rate order of palladation reaction in the concentration of Et_3N and pyridine is -0.25 and -0.39 , respectively (Fig S2 and Fig 2). These negative fractional order reaction rates in the concentration of Et_3N and pyridine suggest that the rate of C–H bond palladation in **7c** and **8c** is actually retarded with the increased concentration of Et_3N and pyridine. Mostlikely, the complexes **7c** and **8c** are stabilized with the high concentration of respective bases by restricting the ligated-base dissociation.

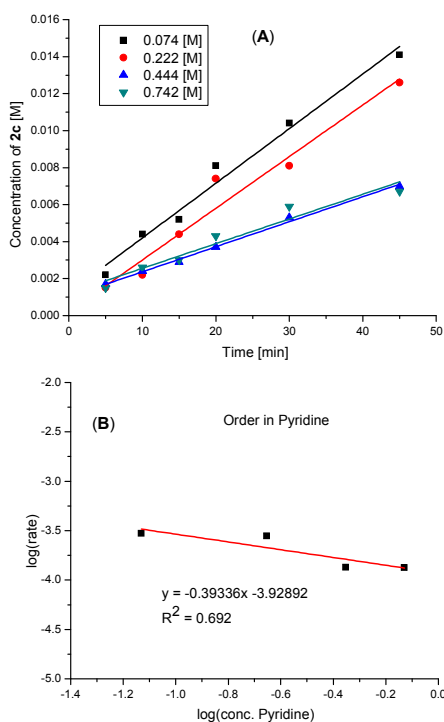
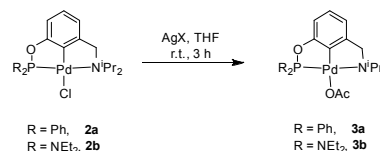


Fig. 2 (A) Time-dependent yields of the palladacycle **2c** at different initial concentration of pyridine. (B) Plot of $\log(\text{rate})$ vs $\log(\text{conc. pyridine})$. The rates are average of two independent measurements.



Scheme 6 Synthesis of POCN-pincer palladium derivatives.

On the basis of all the experimental findings, the pathways for the formation “POCN”-pincer palladium and “PC”-chelate palladacycle can be drawn as shown in Scheme 5. Thus, the formation of pincer complex **2c** occurred *via* the chelate intermediate species **6c** in the presence of an inorganic base K_3PO_4 , whereas the binuclear complex **4c** was formed *via* the Lewis base-coordinated intermediate **7c**. Notably, the Lewis base-coordinated intermediate might leads to the formation of pincer complex (as seen in the case of **8c**), provided the dangling non-coordinated arm ($-\text{CH}_2\text{N}^i\text{Pr}_2$) displaced the coordinated-base (L) and generates the chelate species **6c**. Hence, we proposed that the primary requirement for the synthesis of a chloro-bridged binuclear complex could be the use of a coordinating Lewis base (L); and secondly, the substantial steric hindrance between the coordinated-base and the dangling arm ($-\text{CH}_2\text{N}^i\text{Pr}_2$) to avoid the formation of intermediate **6c**. We assume that the steric between the N-arm ($-\text{CH}_2\text{N}^i\text{Pr}_2$) and coordinated ligand (L) is crucial to the specific palladacycle formation, rather than the electronic factor (Et_3N vs Py). This can be further outlined on the fact that a slightly less bulky ligand $\text{Ph}_2\text{PO}-\text{C}_6\text{H}_4-\text{CH}_2\text{NET}_2$ upon the reaction with PdCl_2 in presence of Et_3N , generated the pincer-ligated palladium complex;^{8b} though the ligand **1c** reacted with $\text{Pd}(\text{COD})\text{Cl}_2$ and Et_3N to produces the non-pincer complex **4c**.

Syntheses of POCN-pincer palladium derivatives

The treatments of (POCN) PdCl complexes **2a** and **2b** with AgOAc in THF at room temperature resulted in the formation of complexes $\{\kappa^P, \kappa^C, \kappa^N-2-(\text{R}_2\text{PO})-\text{C}_6\text{H}_3-6-(\text{CH}_2\text{N}^i\text{Pr}_2)\}\text{Pd}(\text{OAc})$ [R = Ph (**3a**) and R = Et_2N (**3b**)] in good yields (Scheme 6). The ^{31}P NMR spectra of the complexes **3a** and **3b** displayed single resonances at 143.8 and 142.3 ppm, respectively. In the ^1H NMR spectra, the $-\text{OCOCH}_3$ protons appeared as singlets at 1.86 and 1.92 ppm for **3a** and **3b**, respectively. Other ^1H and ^{13}C NMR peaks for the complexes **3a** and **3b** as well as their splitting patterns are largely resembled with that observed in the respective spectra of complexes **2a** and **2b**. Moreover, the MALDI-TOF and elemental analyses of both the complexes are in accord with the assigned molecular structures. The complexes **3a** and **3b** were further characterized by ^{13}C NMR, elemental analyses and single crystal X-ray diffraction studies.

Molecular structures of palladium complexes

The crystals of the complexes **2a**, **2b**, **3a**, **3b** and **5a**, suitable for the X-ray diffraction study were obtained from the slow evaporation of *n*-hexane solution of the complexes at room temperature. The ORTEP diagrams are shown in Fig. 3-7 and the selected bond lengths and bond angles are given in the

respective figure captions. In the structures of **2a** and **2b**, the geometry around the palladium is distorted square planar. The Pd–C bond lengths, 1.9514(16) and 1.960(2) Å in **2a** and **2b**, respectively; are comparable with the Pd–C bond length (1.957(2) Å) in the similar complex (3-MeO-^{Ph}2POCN^{Me})PdCl.^{8d} The Pd–Cl bond length (2.4082(6) Å) in **2b** is slightly longer than the Pd–Cl bond length (2.3848(4) Å) observed in **2a**, which might be due to the σ -donor strength exerted by the (^{Et}2N)²POCN^{iPr}2 moiety upon the palladium in **2b** being stronger than that of the (^{Ph}2POCN^{iPr}2) moiety in complex **2a**. The Pd–P bond length (2.1885(4) Å) in **2a** is comparable with that of the complex (3-MeO-^{Ph}2POCN^{Me})PdCl (Pd–P = 2.1858(6) Å).^{8d} However, the Pd–P bond length (2.1951(6) Å) in **2b** is significantly shorter than the Pd–P bond lengths (2.284(2), 2.277(2) Å) observed in the symmetrical pincer complex (^{Et}2N)⁴POCOPd.⁵ⁿ The Pd(1)–N(1) bond length (2.2032(13) Å) in **2a** is slightly shorter than the Pd(1)–N(1) bond length (2.2204(17) Å) in (^{iPr}2POCN^{iPr}2)PdCl,¹⁴ whereas the Pd(1)–N(1) bond length (2.2361(16) Å) in **2b** is slightly longer than that observed in complex (^{iPr}2POCN^{iPr}2)PdCl. For the complexes **2a** and **2b**, the P–Pd–N bond angles are 161.10(4) and 161.30(5)°, respectively; which are smaller than the corresponding bond angle (P–Pd–N, 162.10(5)°) in the (^{iPr}2POCN^{iPr}2)PdCl complex.¹⁴

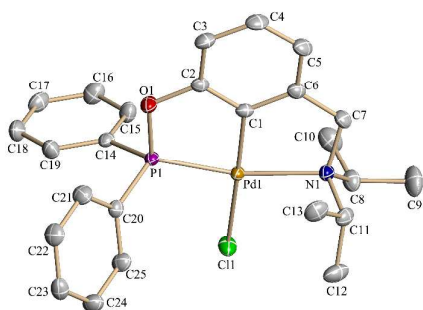


Fig. 3 Thermal ellipsoid plot of (^{Ph}2POCN^{iPr}2)PdCl (**2a**). All the hydrogen atoms are omitted for clarity. Selected bond lengths (Å): Pd(1)–C(1), 1.9514(16); Pd(1)–P(1), 2.1885(4); Pd(1)–N(1), 2.2032(13); Pd(1)–Cl(1), 2.3848(4). Selected bond angles (°): C(1)–Pd(1)–P(1), 80.52(5); C(1)–Pd(1)–N(1), 81.72(6); P(1)–Pd(1)–N(1), 161.10(4); C(1)–Pd(1)–Cl(1), 176.08(5); P(1)–Pd(1)–Cl(1), 98.672(16); N(1)–Pd(1)–Cl(1), 99.48(4).

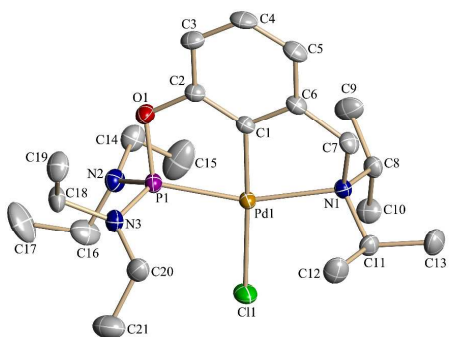


Fig. 4 Thermal ellipsoid plot of (^{Et}2N)²POCN^{iPr}2PdCl (**2b**). All the hydrogen atoms are omitted for clarity. Selected bond lengths (Å): Pd(1)–C(1), 1.960(2); Pd(1)–P(1), 2.1951(6); Pd(1)–N(1), 2.2361(16); Pd(1)–Cl(1), 2.4082(6). Selected bond angles (°): C(1)–Pd(1)–P(1), 80.26(6); C(1)–Pd(1)–N(1), 81.09(8); P(1)–Pd(1)–N(1), 161.30(5); C(1)–Pd(1)–Cl(1), 176.84(6); P(1)–Pd(1)–Cl(1), 97.42(2); N(1)–Pd(1)–Cl(1), 101.27(5).

For the complexes **3a** and **3b**, the coordination geometry around the palladium is slightly distorted from the expected square planar geometry. The acetate ligand in both the complexes binds as η^1 -coordinated fashion, and the Pd–O bond lengths (2.084(2) Å in **3a**, 2.1247(12) Å in **3b**) are similar to those found in other examples of palladium-acetate complexes, wherein the acetate ligand is *trans* to aryl groups.^{5h,18} The Pd–C bond lengths (1.952(3) and 1.9510(17) Å) in **3a** and **3b** are comparable with the Pd–C bond lengths in their halide counterparts **2a** and **2b**, which is in line with the similar *trans* influence of both chloride and acetate ligands. However, the Pd–P bond lengths (2.2136(8) and 2.2140(5) Å) in the **3a** and **3b** are slightly longer than the corresponding Pd–P bond lengths in halide derivatives **2a** and **2b**. The P(1)–Pd(1)–O(2) bond angles in **3a** and **3b** are 102.90(6)° and 102.48(4)°, whereas the N(1)–Pd(1)–O(2) bond angles are 93.34(9)° and 95.14(5)°. This indicates that the O(2) atom of OC(O)CH₃ ligand is aligned more towards N-arm than the P-arm, whereas the carbonyl oxygen O(3) is closer to the P-center than the N-center in both the complexes **3a** and **3b**.

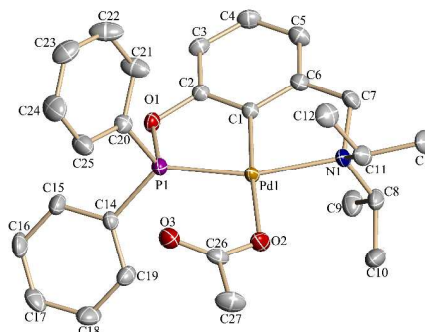


Fig. 5 Thermal ellipsoid plot of (^{Ph}2POCN^{Ph}2)PdOAc (**3a**). All the hydrogen atoms are omitted for clarity. Selected bond lengths (Å): Pd(1)–C(1), 1.952(3); Pd(1)–P(1), 2.2136(8); Pd(1)–N(1), 2.207(2); Pd(1)–O(2), 2.084(2); C(26)–O(2), 1.276(4); C(26)–O(3), 1.243(4). Selected bond angles (°): C(1)–Pd(1)–P(1), 81.21(8); C(1)–Pd(1)–N(1), 82.44(10); P(1)–Pd(1)–N(1), 162.89(6); C(1)–Pd(1)–O(2), 175.64(10); P(1)–Pd(1)–O(2), 102.90(6); N(1)–Pd(1)–O(2), 93.34(9).

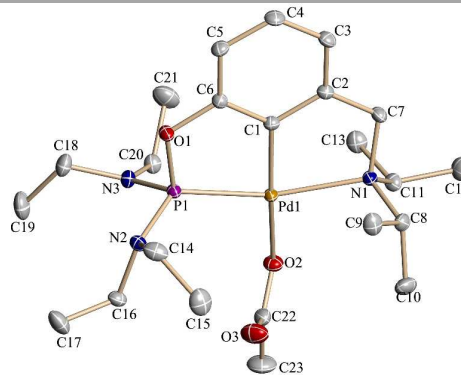


Fig. 6 Thermal ellipsoid plot of (^{Et}2N)²POCN^{iPr}2PdOAc (**3b**). All the hydrogen atoms are omitted for clarity. Selected bond lengths (Å): Pd(1)–C(1), 1.9510(17); Pd(1)–P(1), 2.2140(5); Pd(1)–N(1), 2.2295(14); Pd(1)–O(2), 2.1247(12). Selected bond angles (°): C(1)–Pd(1)–P(1), 80.77(6); C(1)–Pd(1)–N(1), 81.97(7); P(1)–Pd(1)–N(1), 162.35(4); C(1)–Pd(1)–O(2), 170.84(6); P(1)–Pd(1)–O(2), 102.48(4); N(1)–Pd(1)–O(2), 95.14(5).

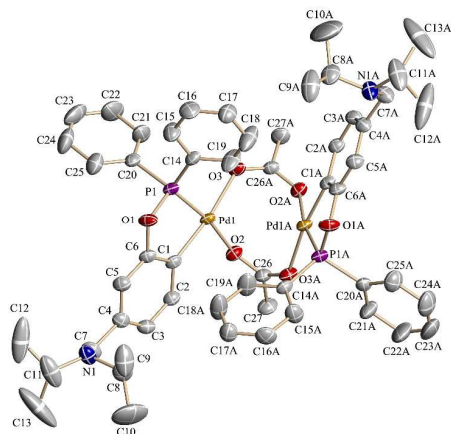


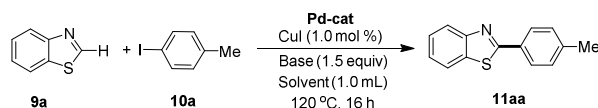
Fig. 7 Thermal ellipsoid plot of complex **5a**. All the hydrogen atoms are omitted for clarity. Selected bond lengths (Å): Pd(1)–C(1), 2.002(4); Pd(1)–P(1), 2.1730(12); Pd(1)–O(2), 2.093(3); Pd(1)–O(3), 2.139(3); C(26)–O(3), 1.249(5); C(26)–O(3A), 1.253(5). Selected bond angles (°): C(1)–Pd(1)–P(1), 79.51(12); C(1)–Pd(1)–O(2), 92.23(15); P(1)–Pd(1)–O(2), 169.83(9); C(1)–Pd(1)–O(3), 171.83(14); P(1)–Pd(1)–O(3), 97.33(9); O(2)–Pd(1)–O(3), 90.06(11).

In the binuclear palladium complex **5a**, each palladium center is ligated with one P-center, one C-center and the third and fourth coordination sites are occupied by the oxygen-atoms of two bridged acetate ligands to form a C_2 -symmetry molecule (Fig. 7). Both the palladium centers are slightly distorted from the expected square planar geometry. The five-membered palladacycle rings containing Pd-, P- and O-atoms are in *transoid* conformation.¹⁷ The eight-membered ring containing two palladium and two acetate ligands form a boat conformation, with both the palladium occupying apical positions. The distance between the two palladium centers is 3.408 Å, which is longer than the sum of their van der Waals' radii (3.26 Å), and hence not considered as a bonding interaction. The Pd–C(1) bond length is 2.002(4) Å, which is slightly longer than the Pd–C bond length (1.952(3) Å) in pincer complex **3a**. The Pd–P(1) bond length (2.1730(12) Å) is significantly shorter than the Pd–P(1) bond length (2.216(1) Å) found in a similar palladacycle binuclear complex.^{3a} The Pd–O(3) bond length (2.139(3) Å) *trans* to the Pd–C is slightly longer than the Pd–O(2) bond length (2.093(3) Å) located in the *cis* position, which could be due to the strong *trans* effect of the carbon compared to the phosphorus-atom ligand. The P–Pd–C bond angle is 79.51(12)°, whereas the O(2)–Pd–O(3) bond angle is a perfect right angle (90.06(11)°).

Catalytic activity of palladacycles for the arylation of azoles

Recently, we have shown that the pincer-based palladium catalyst ($iPr_2POCN^{iPr_2}$)PdCl (**2c**, 0.5 mol%) can be used for the arylation of azoles with aryl iodides, employing CuI (5 mol%) co-catalyst and a relatively expensive Cs_2CO_3 base.¹⁴ Further, it was observed that the sterically less demanding catalyst **2c** is more efficient than a sterically bulky complex ($tBu_2POCN^{iPr_2}$)PdCl. Assuming that the sterically and electronically distinct palladacycles (**2a–5a**) might perform

Table 1 Screening of catalysts and reaction parameters for arylation of azoles^a



Entry	Pd-catalyst	Base	Solvent	Yield (%) ^b
1	2a	K_3PO_4	DMF	59
2	2b	K_3PO_4	DMF	11
3	2c	K_3PO_4	DMF	90 (88)
4	4a	K_3PO_4	DMF	92
5	4b	K_3PO_4	DMF	15
6	4c	K_3PO_4	DMF	95 (93)
7	3a	K_3PO_4	DMF	58
8	3b	K_3PO_4	DMF	4
9	5a	K_3PO_4	DMF	79
10	4c	KOAc	DMF	46
11	4c	K_2CO_3	DMF	50
12	4c	Cs_2CO_3	DMF	46
13	4c	K_3PO_4	DMSO	85 (84)
14	4c	K_3PO_4	DMA	63
15	4c	K_3PO_4	NMP	5
16	4c	K_3PO_4	Toluene	29

^a Reaction conditions: Benzothiazole (0.041 g, 0.3 mmol), 4-iodotoluene (0.098 g, 0.45 mmol), Pd-catalyst (0.5 mol% per Pd), base (0.45 mmol), solvent (1.0 mL). ^b GC yields using *para*-xylene as internal standard, yields in parentheses were that of isolated compounds.

better than **2c**, the newly developed complexes were optimized and employed for the arylation of azoles with aryl iodides using a less expensive K_3PO_4 base and 1.0 mol% of CuI co-catalyst. Initially, all the complexes (**2a–5a**; 0.5 mol% for mononuclear complex, 0.25 mol% for binuclear complexes) were screened for the C–H bond arylation of benzothiazole (**9a**, 0.3 mmol) with 4-iodotoluene (**10a**, 0.45 mmol), employing CuI co-catalyst in the presence of K_3PO_4 in DMF (Table 1, Entries 1–9). Interestingly, the coupled product 2-(*p*-tolyl)benzothiazole (**11aa**) could be obtained in 93% isolated yield, when the binuclear palladacycle **4c** (0.25 mol%) was used as a catalyst in the presence of CuI and K_3PO_4 in DMF (Entry 6). Notably, the palladacycles containing $iPr_2POCN^{iPr_2}$ -ligand backbone (**2c** and **4c**) were shown superior activities than those having $Ph_2POCN^{iPr_2}$ -backbone (**2a**, **3a** and **4a**), whereas the palladacycles with $(Et_2N)_2POCN^{iPr_2}$ -backbone (**2b**, **3b** and **4b**) exhibited very poor catalytic performances (Entries 1–9). The use of Cs_2CO_3 base, which shown to be ideal base for the **2c**-catalyzed arylation, was less efficient with the catalyst **4c**. The arylation reaction in the polar solvents like DMSO and DMA also gave moderate to good yields of coupled product (Entries 13–14).

Having the optimized reaction condition in hand, a number of substituted 5-aryl oxazoles were subjected to the direct arylation with 4-iodotoluene (SI, Table S1, Entries 2–6). Hence, by employing 0.25 mol% of the catalyst **4c** and 1.0 mol% of CuI, the azoles containing electronically different aryl-substituents reacted efficiently with 4-iodotoluene to give the coupled products in good yields. Functional groups like –Cl, – CF_3 and –OMe as well as heteroarene substituent pyridine

were tolerated on the azole substrates. Furthermore, the versatility of the catalyst **4c** in the arylation of azoles with the functionalized aryl iodide electrophiles was tested. Thus, the benzothiazole was very efficiently coupled with the aryl iodides bearing a variety of important functional groups, such as $-OMe$, $-F$, $-Cl$, $-CF_3$ and $-CN$ (Table S1, Entries 7-11). The tolerability of $-F$, $-Cl$ and $-CN$ functional groups in the coupled products (**11ac**, **11ad**, **11af**) are significant, as they could be employed for further functionalization. The aryl iodides having *ortho*-substituents were also employed for the arylation, giving the desired products in moderate to good yields (Entries 14-16). Further, the heteroarene electrophiles also reacted with benzothiazole to produce the coupled products (**11ap**, **11aq**) in moderate yields.

Though, the palladacycle catalyst **4c** showed similar activity as the previously described pincer palladium catalyst **2c** for the arylation of azoles, the excellent performance of the catalyst **4c** in the presence of less expensive base (K_3PO_4) makes this catalyst superior. The C–H bond arylation of azoles were well preceded by *in situ* generated palladium catalysts employing high loading of the precious metal.¹⁹ However, the well-defined palladacycle **4c** catalyzes the arylation of azoles only with 0.25 mol% of the catalyst loading. The mechanistic details for the arylation of azoles catalyzed by the palladacycle **4c** could be interesting to investigate, which is currently underway.

Experimental

General information

All manipulations were conducted under an argon atmosphere either in a glove box or using standard Schlenk techniques in pre-dried glass wares. The catalytic reactions were performed in flame-dried reaction vessels with rubber septa. Solvents were dried over Na/benzophenone or CaH_2 and distilled prior to use. DMF was dried over CaH_2 , distilled under vacuum and stored over 4 Å molecular sieves. Liquid reagents were flushed with argon prior to use. The POCN-H ligand **1c**,¹⁴ 3-((diisopropylamino)methyl)phenol,¹⁴ and 5-aryl azoles²⁰ were synthesized according to previously described procedures. All other chemicals were obtained from commercial sources and were used without further purification. Yields refer to isolated compounds, estimated to be > 95% pure as determined by 1H -NMR. TLC: TLC Silica gel 60 F₂₅₄. Detection under UV light at 254 nm. Chromatography: Separations were carried out on Spectrochem silica gel (0.120-0.250 mm, 60-120 mesh, for organic compounds) and neutral alumina (for inorganic complexes). High resolution mass spectroscopy (HRMS) mass spectra were recorded on a Thermo Scientific Q-Exactive, Accela 1250 pump and MALDI-TOF mass spectra on AB SCIEX TOF/TOFTM 5800/4800 plus. M. p.: Büchi 540 capillary melting point apparatus, values are uncorrected. NMR (1H and ^{13}C) spectra were recorded at 400 or 500 (1H), 100 or 125 (^{13}C , DEPT (distortionless enhancement by polarization transfer)), 377 (^{19}F) and 162 or 202 MHz ($^{31}P\{^1H\}$), respectively on Bruker AV 400 and AV 500 spectrometers in $CDCl_3$ solutions, if not

otherwise specified; chemical shifts (δ) are given in ppm. The 1H and ^{13}C NMR spectra are referenced to residual solvent signals ($CDCl_3$: δ H = 7.26 ppm, δ C = 77.2 ppm) and $^{31}P\{^1H\}$ NMR chemical shifts are referenced to an external standard, H_3PO_4 in D_2O solvent (δ 0.0 ppm), in a sealed capillary tube.

Synthesis of $^{R^2}POCN^{iPr_2}-H$ (R = Ph, **1a**; R = Et₂N, **1b**)

To the suspension of NaH (0.30 g, 12.50 mmol) in THF (10 mL) was added a solution of 3-(diisopropylamino)methyl phenol (2.0 g, 9.65 mmol) in THF (20 mL) and the resulting mixture was refluxed at 70 °C for 3 h. After the reaction mixture was cooled to room temperature, a solution of chlorophosphine, R_2PCl (2.13 g, 9.65 mmol for R = Ph; 2.03 g, 9.65 mmol for R = Et₂N) in THF (20 mL) was added and resulting reaction mixture was further refluxed at 70 °C for 12 h. The reaction mixture was cooled to ambient temperature and volatiles were evaporated under reduced pressure. The compounds were extracted with *n*-hexane (60 mL x 3) and the combined *n*-hexane solutions were evaporated under vacuum to obtain oily products of $^{R^2}POCN^{iPr_2}-H$.

$^{Ph_2}POCN^{iPr_2}-H$ (**1a**): Yield = 3.20 g, 85%. 1H -NMR (500 MHz, $CDCl_3$): δ = 7.61-7.56 (m, 4H, Ar-H), 7.37-7.32 (m, 6H, Ar-H), 7.21 (s, 1H, Ar-H), 7.14 (dd, J = 7.9, 7.6 Hz, 1H, Ar-H), 7.01 (d, J = 7.3 Hz, 1H, Ar-H), 6.95 (d, J = 6.7 Hz, 1H, Ar-H), 3.58 (s, 2H, CH_2), 2.95 (sept, J = 6.7 Hz, 2H, $CH(CH_3)_2$), 0.96 (d, J = 6.4 Hz, 12H, CH_3). ^{13}C -NMR (100 MHz, $CDCl_3$): δ = 157.4 (d, J_{p-c} = 9.0 Hz, C_q), 145.4 (C_q), 141.1 (d, J_{p-c} = 18.2 Hz, 2C, C_q), 130.7 (2C, CH), 130.5 (2C, CH), 129.6 (2C, CH), 129.0 (CH), 128.5 (d, J_{p-c} = 6.4 Hz, 4C, CH), 121.9 (CH), 118.1 (d, J = 10.9, CH), 116.6 (d, J = 10.0 Hz, CH), 48.8 (CH_2), 47.9 (2C, $CH(CH_3)_2$), 20.8 (4C, $CH(CH_3)_2$). $^{31}P\{^1H\}$ -NMR (202 MHz, $CDCl_3$): δ = 109.7 (s).

$^{(Et_2N)_2}POCN^{iPr_2}-H$ (**1b**): Yield = 3.10 g, 84%. 1H -NMR (500 MHz, $CDCl_3$): δ = 7.14 (vt, J = 7.7 Hz, 1H, Ar-H), 7.07 (s, 1H, Ar-H), 6.97 (d, J = 7.3 Hz, 1H, Ar-H), 6.83 (d, J = 7.8 Hz, 1H, Ar-H), 3.60 (s, 2H, CH_2), 3.22-3.10 (m, 4H, CH_2CH_3), 3.09-2.95 (m, 4H, CH_2CH_3 ; 2H, $CH(CH_3)_2$), 1.05 (t, J = 6.8 Hz, 12H, $N(CH_2CH_3)_2$), 1.01 (d, J = 6.6 Hz, 12H, $CH(CH_3)_2$). ^{13}C -NMR (100 MHz, $CDCl_3$): δ = 155.8 (d, J_{p-c} = 7.7 Hz, C_q), 144.9 (C_q), 128.7 (CH), 121.3 (CH), 118.9 (d, J_{p-c} = 10.8 Hz, CH), 117.4 (d, J_{p-c} = 9.3 Hz, CH), 48.9 (CH_2), 47.8 (2C, $CH(CH_3)_2$), 39.1 (d, J_{p-c} = 19.3 Hz, 4C, CH_2CH_3), 20.9 (4C, $CH(CH_3)_2$), 14.8 (d, J_{p-c} = 3.1 Hz, 4C, CH_2CH_3). $^{31}P\{^1H\}$ -NMR (202 MHz, $CDCl_3$): δ = 131.8 (s).

Synthesis of $(^{R^2}POCN^{iPr_2})PdCl$ (R = Ph, **2a**; R = Et₂N, **2b**)

A mixture of $Pd(COD)Cl_2$ (0.058 g, 0.203 mmol for compound **2a**; 0.15 g, 0.525 mmol for compound **2b**), appropriate amount of $(^{R^2}POCN^{iPr_2})-H$ (0.079 g, 0.203 mmol of **1a**; 0.20 g, 0.525 mmol of **1b**) and K_3PO_4 (0.047 g, 0.223 mmol for compound **2a**; 0.122 g, 0.577 mmol for compound **2b**) was taken in a schlenk flask and 1,4-dioxane (20 mL) was added into it. The reaction mixture was heated at 70 °C for 2 h under argon atmosphere. The yellow suspension formed was cooled to ambient temperature, filtered through cannula and the volatile were evaporated under reduced pressure. The crude product was purified by column chromatography using neutral alumina (*n*-hexane/EtOAc : 10/1). The X-ray quality single

crystals were obtained by the slow evaporation of *n*-hexane solution of the compounds at room temperature.

(^{Ph²}POCN^{iPr₂})PdCl (2a): Yield = 0.019 g, 18%. M. p. = 209 °C. ¹H-NMR (500 MHz, CDCl₃): δ = 8.03-7.99 (m, 4H, Ar-H), 7.52-7.44 (m, 6H, Ar-H), 6.98 (dd, *J* = 7.6, 7.3 Hz, 1H, Ar-H), 6.72 (d, *J* = 7.6 Hz, 1H, Ar-H), 6.68 (d, *J* = 7.3 Hz, 1H, Ar-H), 4.14 (s, 2H, CH₂), 3.61 (apparent octet, *J* = 6.1 Hz, 2H, CH(CH₃)₂), 1.69 (d, *J* = 6.1 Hz, 6H, CH(CH₃)₂), 1.23 (d, *J* = 6.1 Hz, 6H, CH(CH₃)₂). ¹³C-NMR (100 MHz, CDCl₃): δ = 162.1 (d, *J*_{P-C} = 10.0 Hz, C_q), 153.6 (C_q), 144.5 (C_q), 133.8 (d, *J*_{P-C} = 54.0 Hz, 2C, C_q), 132.0 (4C, CH), 131.9 (2C, CH), 129.0 (d, *J*_{P-C} = 13.2 Hz, 4C, CH), 126.8 (CH), 115.4 (CH), 109.2 (d, *J*_{P-C} = 17.7 Hz, CH), 61.6 (CH₂), 57.6 (2C, CH(CH₃)₂), 22.8 (2C, CH(CH₃)₂), 19.7 (2C, CH(CH₃)₂). ³¹P{¹H}NMR (202 MHz, CDCl₃): δ = 150.0 (s). MALDI-TOF: *m/z* calcd for C₂₅H₂₉ClNOPd-Cl⁺ [M-Cl]⁺ 496.1022; found 496.1617. Anal. calcd for C₂₅H₂₉ClNOPd: C, 56.40; H, 5.49; N, 2.63. Found: C, 55.84; H, 5.41; N, 2.23.

(^{Et₂N})₂POCN^{iPr₂})PdCl (2b): Yield = 0.079 g, 29%. M. p. = 105 °C. ¹H-NMR (500 MHz, CDCl₃): δ = 6.94 (dd, *J* = 7.9, 7.6 Hz, 1H, Ar-H), 6.63 (d, *J* = 7.3 Hz, 1H, Ar-H), 6.55 (d, *J* = 7.9 Hz, 1H, Ar-H), 4.01 (s, 2H, CH₂), 3.52 (apparent octet, *J* = 6.4 Hz, 2H, CH(CH₃)₂), 3.36-3.22 (m, 8H, CH₂CH₃), 1.62 (d, *J* = 6.4 Hz, 6H, CH(CH₃)₂), 1.17-1.13 (m, 6H, CH(CH₃)₂; 12H, (CH₂CH₃)₄). ¹³C-NMR (100 MHz, CDCl₃): δ = 157.5 (d, *J*_{P-C} = 15.4 Hz, C_q), 153.6 (d, *J*_{P-C} = 2.3 Hz, C_q), 143.1 (d, *J*_{P-C} = 2.3 Hz, C_q), 126.6 (CH), 115.0 (CH), 108.2 (d, *J*_{P-C} = 19.3 Hz, CH), 60.7 (d, *J*_{P-C} = 2.3 Hz, CH₂), 57.0 (d, *J*_{P-C} = 3.1 Hz, 2C, CH(CH₃)₂), 40.3 (d, *J*_{P-C} = 9.3 Hz, 4C, CH₂CH₃), 22.6 (2C, CH(CH₃)₂), 19.5 (2C, CH(CH₃)₂), 14.4 (d, *J*_{P-C} = 2.3 Hz, 4C, CH₂CH₃). ³¹P{¹H}NMR (202 MHz, CDCl₃): δ = 142.3 (s). MALDI-TOF: *m/z* calcd for C₂₁H₃₉ClN₃OPd-Cl⁺ [M-Cl]⁺ 486.1866; found 486.2410. Anal. calcd for C₂₁H₃₉ClN₃OPd: C, 48.28; H, 7.53; N, 8.04. Found: C, 48.22; H, 7.60; N, 7.62.

Representative procedure for synthesis of (^{R²}POCN^{iPr₂})Pd(OAc)

Synthesis of (^{Ph²}POCN^{iPr₂})Pd(OAc) (3a): To the mixture of 2,6-(Ph₂PO)(C₆H₃)(CH₂-N^{iPr₂})PdCl, **2a** (0.020 g, 0.038 mmol) and AgOAc (0.008 g, 0.046 mmol) was added THF (10 mL) and the reaction mixture was stirred at room temperature for 3 h. The solvent was evaporated under reduced pressure and the compound was extracted with Et₂O (10 mL x 3). Upon evaporation of diethyl ether, the compound **3a** was obtained as a light yellow solid. The compound **3a** was recrystallized from *n*-hexane solution by slow evaporation to obtain X-ray quality single crystals. Yield = 0.013 g, 62%. M. p. = 182 °C. ¹H-NMR (400 MHz, CDCl₃): δ = 7.90-7.84 (m, 4H, Ar-H), 7.49-7.40 (m, 6H, Ar-H), 6.92 (vt, *J* = 7.8 Hz, 1H, Ar-H), 6.61 (d, *J* = 7.3 Hz, 1H, Ar-H), 6.57 (d, *J* = 8.1 Hz, 1H, Ar-H), 4.16 (s, 2H, CH₂), 3.53 (apparent octet, *J* = 6.1 Hz, 2H, CH(CH₃)₂), 1.86 (s, 3H, COCH₃), 1.60 (d, *J* = 6.4 Hz, 6H, CH(CH₃)₂), 1.28 (d, *J* = 6.6 Hz, 6H, CH(CH₃)₂). ¹³C-NMR (100 MHz, CDCl₃): δ = 175.0 (CO), 162.3 (d, *J*_{P-C} = 11.0 Hz, C_q), 153.2 (C_q), 143.0 (C_q), 135.4 (d, *J*_{P-C} = 58.6 Hz, 2C, C_q), 132.7 (d, *J*_{P-C} = 13.4 Hz, 4C, CH), 131.2 (d, *J*_{P-C} = 2.3 Hz, 2C, CH), 128.3 (d, *J*_{P-C} = 12.1 Hz, 4C, CH), 126.4 (CH), 114.5 (CH), 108.6 (d, *J*_{P-C} = 16.6 Hz), 61.4 (CH₂), 57.3 (2C, CH(CH₃)₂), 31.1 (COCH₃), 22.2 (2C, CH(CH₃)₂), 19.5 (2C, CH(CH₃)₂). ³¹P{¹H}NMR (202 MHz, CDCl₃): δ = 143.8 (s). MALDI-TOF: *m/z* calcd for C₂₇H₃₂NO₃PPd-OAc⁺ [M-OAc]⁺ 496.1022; found

496.1594. Anal. calcd for C₂₇H₃₂NO₃PPd: C, 58.33; H, 5.80; N, 2.52. Found: C, 58.42; H, 6.20; N, 1.84.

Synthesis of (^{Et₂N})₂POCN^{iPr₂})Pd(OAc) (3b): The representative procedure was followed, using **2b** (0.058 g, 0.111 mmol) and AgOAc (0.022 g, 0.133 mmol). Yield = 0.040 g, 66%. M. p. = 86 °C. ¹H-NMR (500 MHz, CDCl₃): δ = 6.93 (vt, *J* = 7.7, 1H, Ar-H), 6.59 (d, *J* = 7.5, 1H, Ar-H), 6.53 (d, *J* = 7.7 Hz, 1H, Ar-H), 4.02 (s, 2H, CH₂), 3.38 (apparent octet, *J* = 6.2 Hz, 2H, CH(CH₃)₂), 3.32-3.21 (m, 8H, CH₂CH₃), 1.92 (s, 3H, COCH₃), 1.53 (d, *J* = 6.4 Hz, 6H, CH(CH₃)₂), 1.23 (d, *J* = 6.4 Hz, 6H, CH(CH₃)₂), 1.13 (t, *J* = 7.0 Hz, 12H, CH₂CH₃). ¹³C-NMR (125 MHz, CDCl₃): δ = 175.9 (CO), 157.7 (d, *J*_{P-C} = 14.3 Hz, C_q), 153.6 (d, *J*_{P-C} = 1.9 Hz, C_q), 140.6 (C_q), 126.3 (CH), 114.6 (CH), 108.0 (d, *J*_{P-C} = 19.1 Hz, CH), 60.4 (d, *J*_{P-C} = 2.9 Hz, CH₂), 56.8 (d, *J*_{P-C} = 2.9 Hz, 2C, CH(CH₃)₂), 40.4 (d, *J*_{P-C} = 10.5 Hz, 4C, CH₂CH₃), 24.7 (COCH₃), 21.9 (2C, CH(CH₃)₂), 19.3 (2C, CH(CH₃)₂), 14.4 (d, *J*_{P-C} = 2.9 Hz, 4C, CH₂CH₃). ³¹P{¹H}NMR (202 MHz, CDCl₃): δ = 142.3 (s). MALDI-TOF: *m/z* calcd for C₂₃H₄₂N₃O₃PPd-OAc⁺ [M-OAc]⁺ 486.1866; found 486.2420. Anal. calcd for C₂₃H₄₂N₃O₃PPd: C, 50.60; H, 7.75; N, 7.70. Found: C, 52.37; H, 8.35; N, 6.80.²¹

Procedure for synthesis of [^{κ^P, κ^C-4-^{iPr₂}NCH₂-C₆H₃-Pd(μ-Cl)-(2-OPR₂)₂ (R = Ph, **4a**; R = Et₂N, **4b**; R = ^{iPr}, **4c**)}

A mixture of Pd(COD)Cl₂ (0.306 g, 1.07 mmol for **4a**; 0.550 g, 1.93 mmol for **4b**; 0.088 g, 0.308 mmol for **4c**), (^{R²}POCN^{iPr₂})-H (0.420 g, 1.07 mmol of **1a**; 0.735 g, 1.93 mmol of **1b**; 0.100 g, 0.309 mmol of **1c**) and Et₃N (0.18 mL, 1.28 mmol for **4a**; 0.32 mL, 2.30 mmol for **4b**; 0.05 mL, 0.370 mmol for **4c**) was taken in a schlenk flask and 1,4-dioxane (30 mL) was added into it. The reaction mixture was heated at 70 °C for 2 h under argon atmosphere. The yellow suspension formed was cooled to ambient temperature and the volatile were evaporated under reduced pressure. The compounds was purified by column chromatography on neutral alumina (*n*-hexane:EtOAc / 10:1) to yielded the desired complexes (**4a**, **4b**, **4c**) as light yellow solid.

[^{κ^P, κ^C-4-^{iPr₂}NCH₂-C₆H₃-Pd(μ-Cl)-(2-OPPh₂)₂ (4a):} Yield = 0.138 g, 24%. M.p. = 114-116 °C. ¹H-NMR (500 MHz, CDCl₃): δ = 8.02-7.76 (m, 8H, Ar-H), 7.57-7.35 (m, 14H, Ar-H), 6.99 (br s, 2H, Ar-H), 6.83 (br s, 2H, Ar-H), 3.55 (s, 4H, CH₂), 3.00 (br s, 4H, CH(CH₃)₂), 1.00 (br s, 24H, CH(CH₃)₂). ¹³C-NMR (100 MHz, CDCl₃): δ = 164.3 (2C, C_q), 143.3 (2C, C_q), 135.8 (2C, CH), 132.8 (4C, C_q), 132.5 (4C, CH), 132.3 (d, *J*_{P-C} = 13.6 Hz, 8C, CH), 132.1 (2C, C_q), 129.0 (d, *J*_{P-C} = 10.9 Hz, 8C, CH), 122.0 (2C, CH), 111.4 (2C, CH), 48.7 (2 CH₂), 47.9 (4C, CH(CH₃)₂), 20.9 (8C, CH(CH₃)₂). ³¹P{¹H}NMR (202 MHz, CDCl₃): δ = 152.9 (s, major, 57%), 152.2 (s, minor, 43%). MALDI-TOF: *m/z* calcd for C₅₀H₅₈Cl₂N₂O₂P₂Pd₂+H⁺ [M+H]⁺ 1063.1498; found 1063.3624. Anal. calcd for C₅₀H₅₈Cl₂N₂O₂P₂Pd₂: C, 56.40; H, 5.49; N, 2.63. Found: C, 55.22; H, 5.15; N, 2.25.²¹

[^{κ^P, κ^C-4-^{iPr₂}NCH₂-C₆H₃-Pd(μ-Cl)-(2-OP(NEt₂)₂)₂ (4b):} Yield = 0.320 g, 32%. M. p. = 188-190 °C. ¹H-NMR (500 MHz, CDCl₃): δ = 7.47 (dd, *J* = 6.8, 6.5 Hz, 2H, Ar-H), 6.89-6.77 (m, 4H, Ar-H), 3.55 (s, 4H, CH₂), 3.48-3.34 (m, 8H, CH₂CH₃), 3.29-3.17 (m, 8H, CH₂CH₃), 3.04-2.96 (m, 4H, CH(CH₃)₂), 1.17 (t, *J* = 7.0 Hz, 24H, CH₂CH₃), 1.00 (d, *J* = 6.0, 24H, CH(CH₃)₂). ¹³C-NMR (100 MHz, CDCl₃): δ = 158.3 (d, *J*_{P-C} = 18.1 Hz, 2C, C_q), 142.4 (2C, C_q), 136.1

(2C, CH), 132.5 (2C, C_q), 121.5 (2C, CH), 110.7 (d, $J_{p-c} = 20.9$, 2C, CH), 48.7 (2 CH₂), 47.8 (4C, CH(CH₃)₂), 40.5 (d, $J_{p-c} = 9.1$ Hz, 8C, CH₂CH₃), 20.9 (8C, CH(CH₃)₂), 14.3 (8C, CH₂CH₃). ³¹P{¹H}-NMR (202 MHz, CDCl₃): δ = 137.7 (s, major, 76%), 137.9 (s, minor, 24%). MALDI-TOF: *m/z* calcd for C₄₂H₇₈Cl₂N₆O₂P₂Pd₂+H⁺ [M+H]⁺ 1043.3186; found 1043.4058. Anal. calcd for C₄₂H₇₈Cl₂N₆O₂P₂Pd₂: C, 48.28; H, 7.53; N, 8.04. Found: C, 47.62; H, 7.59; N, 6.86.²¹

[κ^P, κ^C-4-ⁱPr₂NCH₂-C₆H₃-Pd(μ-Cl)-(2-OPⁱPr₂)]₂ (**4c**): Yield: 0.102 g, 71%. M.p. = 153-154 °C. ¹H-NMR (400 MHz, CDCl₃): δ = 7.60-7.36 (m, 2H, Ar-H), 6.90-9.74 (m, 4H, Ar-H), 3.54 (br s, 4H, CH₂), 3.01 (br s, 4H, N{CH(CH₃)₂})₂, 2.41 (br s, 4H, P{CH(CH₃)₂})₂, 1.44 (d, $J = 12.7$ Hz, 12H, PCH(CH₃)₂), 1.31 (dd, $J = 15.9, 6.9$ Hz, 12H, PCH(CH₃)₂), 1.01 (br s, 24H, NCH(CH₃)₂). ¹³C-NMR (100 MHz, CDCl₃): δ = 165.5 (d, $J_{p-c} = 6.2$ Hz, 2C, C_q), 142.8 (2C, C_q), 135.8 (2C, CH), 131.9 (2C, C_q), 121.6 (2C, CH), 110.5 (d, $J_{p-c} = 16.2$ Hz, 2C, CH), 48.7 (2C, CH₂), 47.8 (4C, N{CH(CH₃)₂})₂, 29.5 (d, $J_{p-c} = 29.3$ Hz, 4C, P{CH(CH₃)₂})₂, 20.9 (4C, PCH(CH₃)₂), 17.8 (4C, PCH(CH₃)₂), 17.0 (8C, NCH(CH₃)₂). ³¹P{¹H}-NMR (202 MHz, CDCl₃): δ = 200.0 (s, major, 65%), 199.0 (s, minor, 35%). MALDI-TOF: *m/z* calcd for C₃₈H₆₆Cl₂N₂O₂P₂Pd₂+H [M+H]⁺ 927.2124; found 927.3241. Anal. calcd for C₃₈H₆₆Cl₂N₂O₂P₂Pd₂: C, 49.15; H, 7.16; N, 3.02. Found: C, 49.12; H, 7.34; N, 2.69.

Synthesis of [κ^P, κ^C-4-ⁱPr₂NCH₂-C₆H₃-Pd(μ-OAc)-(2-OPPh₂)]₂ (**5a**)

To the mixture of **4a** (0.040 g, 0.038 mmol) and AgOAc (0.014 g, 0.084 mmol) was added THF (10 mL) and the reaction mixture was stirred at room temperature for 3 h. The solvent was evaporated under reduced pressure and the compound was extracted with Et₂O (10 mL x 3). Upon evaporation of diethyl ether, the compound **5a** was obtained as a light yellow solid. The compound **5a** was further recrystallized from *n*-hexane solution to obtain X-ray quality crystals at room temperature. Yield = 0.024 g, 57%. M. p. = 192 °C. ¹H-NMR (400 MHz, CDCl₃): δ = 7.89-7.70 (m, 6H, Ar-H), 7.51-7.04 (m, 16H, Ar-H), 6.84 (br s, 2H, Ar-H), 6.66 (d, $J = 7.6$ Hz, 2H, Ar-H), 3.55 (s, 4H, CH₂), 3.05 (sept, $J = 6.4$ Hz, 4H, CH(CH₃)₂), 2.17 (s, 6H, COCH₃), 1.04 (d, $J = 6.4$ Hz, 24H, CH(CH₃)₂). ¹³C-NMR (100 MHz, CDCl₃): δ = 181.4 (2C, C_q), 164.5 (d, $J_{p-c} = 14.6$ Hz, 2C, C_q), 141.9 (2C, C_q), 134.7 (2C, CH), 132.6-131.2 (m, 20C), 128.6-128.3 (m, 6C), 121.8 (2C, CH), 111.0 (2C, CH), 48.7 (2C, CH₂), 47.6 (4C, CH(CH₃)₂), 25.4 (2C, COCH₃), 21.0 (8C, CH(CH₃)₂). ³¹P{¹H}-NMR (202 MHz, CDCl₃): δ = 151.0 (s). HRMS (ESI): *m/z* calcd for C₅₄H₆₆N₂O₆P₂Pd₂+H [M+H]⁺ 1113.2539; found 1113.2501. Anal. calcd for C₅₄H₆₆N₂O₆P₂Pd₂: C, 58.23; H, 5.97; N, 2.51. Found: C, 57.69; H, 6.02; N, 2.13.

Synthesis of {κ^P, κ^C-(3-ⁱPr₂NCH₂)-C₆H₄-(2-OPⁱPr₂)}(Py)PdCl₂ (**8c**)

A mixture of Pd(COD)Cl₂ (0.044 g, 0.154 mmol), **1c** (0.050 g, 0.155 mmol) and pyridine (0.015 mL, 0.185 mmol) was taken in a schlenk flask and 1,4-dioxane (10 mL) was added into it. The reaction mixture was stirred at room temperature for 1 h under argon atmosphere and the volatiles were evaporated under reduced pressure to obtain light-yellow compound of **8c**. Yield: 0.065 g, 73%. ¹H-NMR (500 MHz, C₆D₆): δ = 9.08 (br s, 2H, Py-H), 7.99 (s, 1H, Ar-H), 7.62 (d, $J = 7.3$ Hz, 1H, Ar-H),

7.15 (t, $J = 7.9$ Hz, 1H, Ar-H), 7.07 (d, $J = 7.3$ Hz, 1H, Ar-H), 6.67 (br s, 1H, Py-H), 6.40 (br s, 2H, Py-H), 3.55 (s, 2H, CH₂), 2.96 (sept, $J = 6.7$ Hz, 2H, NCH(CH₃)₂), 2.86 (app octet, $J = 7.6$ Hz, 2H, PCH(CH₃)₂), 1.48 (dd, $J = 18.0, 7.3$ Hz, 6H, PCH(CH₃)₂), 1.40 (dd, $J = 16.2, 7.0$ Hz, 6H, PCH(CH₃)₂), 0.95 (d, $J = 6.7, 12$ Hz, NCH(CH₃)₂). ¹³C-NMR (125 MHz, C₆D₆): δ = 155.5 (d, $J_{p-c} = 8.6$ Hz, C_q), 151.6 (CH), 145.7 (C_q), 137.9 (CH), 129.4 (CH), 128.7 (2C, CH), 124.3 (CH), 123.7 (CH), 120.6 (d, $J_{p-c} = 5.7$ Hz, CH), 118.9 (d, $J_{p-c} = 5.7$ Hz, CH), 49.5 (CH₂), 48.5 (2C, NCH(CH₃)₂), 31.5 (d, $J_{p-c} = 31.5$ Hz, 2C, PCH(CH₃)₂), 21.3 (4C, NCH(CH₃)₂), 19.2 (2C, PCH(CH₃)₂), 18.0 (2C, PCH(CH₃)₂). ³¹P{¹H}-NMR (202 MHz, C₆D₆): δ = 144.4 (s). HRMS (ESI): *m/z* calcd for C₂₄H₃₉Cl₂N₂OPPd+H [M+H]⁺ 579.1285; Found 579.1282.

Representative procedure for the arylation of azoles: synthesis of 2-(*p*-tolyl)benzo[*d*]thiazole (**11aa**)

To a flame-dried screw-capped Schlenk tube equipped with magnetic stir bar was introduced CuI in CH₃CN [0.0006 g, 0.003 mmol, 1.0 mol%, 0.1 mL from the stock solution (0.036 g in CH₃CN (6.0 mL))] and the solvent was evaporated to dryness under vacuum. Then, 4-iodotoluene **10a** (0.098 g, 0.45 mmol), K₃PO₄ (0.096 g, 0.45 mmol) and benzothiazole **9a** (0.041 g, 0.30 mmol) were added under argon. The screw-capped Schlenk tube with the mixture was then evacuated and refilled with argon. To the above mixture was added Pd-catalyst **4c** (0.00075 mmol, 0.25 mol% (0.5 mol% per Pd), 1.0 mL of 0.00075 M stock solution in DMF) in DMF under argon. The resultant reaction mixture was then stirred at 120 °C in a pre-heated oil bath for 16 h. At ambient temperature, H₂O (10 mL) was added and the reaction mixture was extracted with EtOAc (15 mL x 3). The combined organic layers were dried over MgSO₄ and the solvent was evaporated *in vacuo*. The remaining residue was purified by column chromatography on silica gel (*n*-hexane/EtOAc 30/1 → 20/1) to yield **11aa** (0.063 g, 93%) as an off-white solid.

All the isolated coupled products (**11aa-11aq**) were characterized by ¹H and ¹³C-NMR techniques and well compared with the literature reports.

X-ray structure determination

X-ray intensity data measurements of compounds **2a**, **2b**, **3a**, **3b** and **5a** were carried out on a Bruker SMART APEX II CCD diffractometer with graphite-monochromatized (MoK_α = 0.71073 Å) radiation between 150(2) - 296 (2) K. The X-ray generator was operated at 50 kV and 30 mA. A preliminary set of cell constants and an orientation matrix were calculated from three sets of 12 frames (total 36 frames). Data were collected with ω scan width of 0.5° at eight different settings of φ and 2θ with a frame time of 10 sec keeping the sample-to-detector distance fixed at 5.00 cm for all the compounds. The X-ray data collection was monitored by APEX2 program (Bruker, 2006).²² All the data were corrected for Lorentzian, polarization and absorption effects using SAINT and SADABS programs (Bruker, 2006). SHELX-97 was used for structure solution and full matrix least-squares refinement on F².²³ Hydrogen atoms were placed in geometrically idealized

position and constrained to ride on their parent atoms. CCDC-1063772 (**2a**), CCDC-1063769 (**2b**), CCDC-1063773 (**3a**), CCDC-1063770 (**3b**) and CCDC-1063774 (**5a**) contain the supplementary crystallographic data.

Conclusions

In summary, two unsymmetrical POCN ligands, and a series of mononuclear pincer palladium complexes and chloro-bridged binuclear palladacycles have been synthesized *via* the regioselective C–H bond activation of the POCN–H ligands. Thus, the palladation reactions of the POCN–H ligands bearing isopropyl substituents on N-atom produced “PC”-palladacycles **4a–4c** in the presence of Et₃N, whereas the same ligands in the presence of K₃PO₄ or pyridine afford “POCN”-pincer palladium complexes; *via* the selective activation of the arene C(4)–H and C(2)–H bond, respectively. Mechanistic studies on the C–H bond palladation of POCN–H ligand suggests that the regioselectivity was dictated by the coordinating ability of the external base as well as the steric between the base and nitrogen-ligand arm, rather than the electronic parameters between them. The impact of the employed base on the regioselective palladation was insignificant, when an electrophilic palladium precursor Pd(OAc)₂ is employed instead of Pd(COD)Cl₂. All the palladacycles were fully characterized by multinuclear NMR studies and the molecular structures of many complexes were established by X-ray crystal structure determination. The palladacycle **4c** shows excellent catalytic activity for the arylation of azoles with aryl iodides employing a relatively moderate and inexpensive base K₃PO₄, under the mild reaction conditions. Mechanistic detail, including kinetic studies and DFT calculations, to understand the pathway for the **4c**-catalyzed arylation of azoles is currently underway.

Acknowledgements

This work was financially supported by DST, New Delhi (SR/S1/IC-42/2012) and CSIR-New Delhi (Network project ORIGIN, CSC0108). D.K.P. thanks UGC, New Delhi for a research fellowship. We thank Dr. P. R. Rajmohan for NMR facility and Dr. (Mrs) Shanthakumari for HRMS analyses.

Notes and references

- (a) M. Albrecht and G. van Koten, *Angew. Chem. Int. Ed.*, 2001, **40**, 3750-3781; (b) J. Dupont, C. S. Consorti and J. Spencer, *Chem. Rev.*, 2005, **105**, 2527-2572.
- For selected reviews, see: (a) W. A. Herrmann, V. P. W. Böhm and C.-P. Reisinger, *J. Organomet. Chem.*, 1999, **576**, 23-41; (b) J. Dupont, M. Pfeiffer and J. Spencer, *Eur. J. Inorg. Chem.*, 2001, 1917-1927; (c) R. B. Bedford, *Chem. Commun.*, 2003, 1787-1796; (d) M. E. van der Boom and D. Milstein, *Chem. Rev.*, 2003, **103**, 1759-1792; (e) J. T. Singleton, *Tetrahedron*, 2003, **59**, 1837-1857; (f) I. P. Beletskaya and A. V. Cheprakov, *J. Organomet. Chem.*, 2004, **689**, 4055-4082; (g) I. Omae, *Coord. Chem. Rev.*, 2004, **248**, 995-1023; (h) R. B. Bedford, C. S. J. Cazin and D. Holder, *Coord. Chem. Rev.*, 2004, **248**, 2283-2321; (i) N. Selander and K. Szabó, *Chem. Rev.*, 2011, **111**,

- 2048-2076; (j) K. J. Szabó *Top Organomet. Chem.*, 2013, **40**, 203-242.
- For some specific examples, see: (a) W. A. Herrmann, C. Brossmer, K. Öfele, C.-P. Reisinger, T. Priermeier, M. Beller and H. Fischer, *Angew. Chem. Int. Ed. Engl.*, 1995, **34**, 1844-1848; (b) M. Beller, H. Fischer, W. A. Herrmann, K. Öfele and C. Brossmer, *Angew. Chem. Int. Ed. Engl.*, 1995, **34**, 1848-1849; (c) R. B. Bedford, S. M. Draper, P. Noelle Scully and S. L. Welch, *New J. Chem.*, 2000, **24**, 745-747; (d) D. Morales-Morales, R. Redon, C. Yung and C. M. Jensen, *Chem. Commun.*, 2000, 1619-1620; (e) J. Lu, J. Ye and W.-L. Duan, *Org. Lett.*, 2013, **15**, 5016-5019; (f) B. Ding, Z. Zhang, Y. Liu, M. Sugiya, T. Imamoto and W. Zhang, *Org. Lett.*, 2013, **15**, 3690-3693; (g) A. Rossin, G. Bottari, A. M. Lozano-Vila, M. Paneque, M. Peruzzini, A. Rossi and F. Zanobini, *Dalton Trans.*, 2013, **42**, 3533-3541; (h) A. Bruneau, M. Roche, M. Alami and S. Messaoudi, *ACS Catal.*, 2015, **5**, 1386-1396.
- (a) M.-C. Lagunas, R. A. Gossage, A. L. Spek and G. van Koten, *Organometallics*, 1998, **17**, 731-741; (b) I. G. Jung, S. U. Son, K. H. Park, K.-C. Chung, J. W. Lee and Y. K. Chung, *Organometallics*, 2003, **22**, 4715-4720; (c) M. Q. Slagt, G. Rodríguez, M. M. P. Grutters, R. J. M. Klein Gebbink, W. Klopffer, L. W. Jenneskens, M. Lutz, A. L. Spek and G. van Koten, *Chem. Eur. J.*, 2004, **10**, 1331-1344; (d) K. Takenaka and Y. Uozumi, *Org. Lett.*, 2004, **6**, 1833-1835; (e) A. J. Canty, M. C. Denney, G. van Koten, B. W. Skelton and A. H. White, *Organometallics*, 2004, **23**, 5432-5439; (f) K. Takenaka and Y. Uozumi, *Adv. Synth. Catal.*, 2004, **346**, 1693-1696; (g) J. Kjellgren, H. Sundén and K. J. Szabó, *J. Am. Chem. Soc.*, 2004, **126**, 474-475. (h) B. Soro, S. Stoccoro, G. Minghetti, A. Zucca, M. A. Cinellu, S. Gladiali, M. Manassero and M. Sansoni, *Organometallics*, 2005, **24**, 53-61; (i) K. Takenaka, M. Minakawa and Y. Uozumi, *J. Am. Chem. Soc.*, 2005, **127**, 12273-12281; (j) J. Kjellgren, H. Sundén and K. J. Szabó, *J. Am. Chem. Soc.*, 2005, **127**, 1787-1796; (k) B. Soro, S. Stoccoro, G. Minghetti, A. Zucca, M. A. Cinellu, M. Manassero and S. Gladiali, *Inorg. Chim. Acta*, 2006, **359**, 1879-1888; (l) M. S. Yoon, R. Ramesh, J. Kim, D. Ryu and K. H. Ahn, *J. Organomet. Chem.*, 2006, **691**, 5927-5934; (m) N. Selander, B. Willy and K. J. Szabó, *Angew. Chem. Int. Ed.*, 2010, **49**, 4051-4053; (n) S. Nakamura, K. Hyodo, M. Nakamura, D. Nakane and H. Masuda, *Chem. Eur. J.*, 2013, **19**, 7304-7309; (o) K. Hyodo, M. Kondo, Y. Funahashi and S. Nakamura, *Chem. Eur. J.*, 2013, **19**, 4128-4134.
- (a) C. J. Moulton and B. L. Shaw, *J. Chem. Soc., Dalton Trans.*, 1976, 1020-1024; (b) M. Ohff, A. Ohff, M. E. van der Boom and D. Milstein, *J. Am. Chem. Soc.*, 1997, **119**, 11687-11688; (c) D. Morales-Morales, C. Grause, K. Kasaoka, R. Redón, R. E. Cramer and C. M. Jensen, *Inorg. Chim. Acta*, 2000, **300-302**, 958-963; (d) M. R. Eberhard, Z. Wang and C. M. Jensen, *Chem. Commun.*, 2002, 818-819; (e) M. R. Eberhard, S. Matsukawa, Y. Yamamoto and C. M. Jensen, *J. Organomet. Chem.*, 2003, **687**, 185-189; (f) O. A. Wallner and K. J. Szabó, *Org. Lett.*, 2004, **6**, 1829-1831; (g) A. Naghypour, S. J. Sabounchei, D. Morales-Morales, S. Hernández-Ortega and C. M. Jensen, *J. Organomet. Chem.*, 2004, **689**, 2494-2502; (h) R. Johansson, M. Jarenmark and O. F. Wendt, *Organometallics*, 2005, **24**, 4500-4502; (i) D. Olsson, P. Nilsson, M. El Masnaouy and O. F. Wendt, *Dalton Trans.*, 2005, 1924-1929; (j) P. A. Chase, M. Gagliardo, M. Lutz, A. L. Spek, G. P. M. van Klink and G. van Koten, *Organometallics*, 2005, **24**, 2016-2019; (k) D. Benito-Garagorri, V. Bocokić, K. Mereiter and K. Kirchner, *Organometallics*, 2006, **25**, 3817-3823; (l) M. C. Denney, N. A. Smythe, K. L. Cetto, R. A. Kemp and K. I. Goldberg, *J. Am. Chem. Soc.*, 2006, **128**, 2508-2509; (m) R. A. Baber, R. B. Bedford, M. Betham, M. E. Blake, S. J. Coles, M. F. Haddow, M. B. Hursthouse, A. G. Orpen, L. T. Pilarski, P. G. Pringle and R. L. Wingad, *Chem. Commun.*,

- 2006, 3880-3882; (n) T. Kimura and Y. Uozumi, *Organometallics*, 2006, **25**, 4883-4887; (o) F. Churruca, R. SanMartin, I. Tellitu and E. Domínguez, *Tetrahedron Lett.*, 2006, **47**, 3233-3237; (p) J. L. Bolliger, O. Blacque and C. M. Frech, *Angew. Chem. Int. Ed.*, 2007, **46**, 6514-6517; (q) R. Johansson and O. F. Wendt, *Dalton Trans.*, 2007, 488-492; (r) R. Johansson and O. F. Wendt, *Organometallics*, 2007, **26**, 2426-2430; (s) A. Naghypour, S. J. Sabounchei, D. Morales-Morales, D. Canseco-González and C. M. Jensen, *Polyhedron*, 2007, **26**, 1445-1448; (t) J. Aydin and K. J. Szabó, *Org. Lett.*, 2008, **10**, 2881-2884; (u) R. Gerber, O. Blacque and C. M. Frech, *ChemCatChem*, 2009, **1**, 393-400; (v) M. M. Konnick, N. Decharin, B. V. Popp and S. S. Stahl, *Chem. Sci.*, 2011, **2**, 326-330; (w) D. Duncan, E. G. Hope, K. Singh and A. M. Stuart, *Dalton Trans.*, 2011, **40**, 1998-2005; (x) A. Adhikary, J. R. Schwartz, L. M. Meadows, J. A. Krause and H. Guan, *Inorg. Chem. Front.*, 2014, **1**, 71-82.
6. (a) N. Lucena, J. Casabó, L. Escriche, G. Sánchez-Castelló, F. Teixidor, R. Kivekäs and R. Sillanpää, *Polyhedron*, 1996, **15**, 3009-3018; (b) T. Kanbara and T. Yamamoto, *J. Organomet. Chem.*, 2003, **688**, 15-19; (c) M. D. Meijer, B. Mulder, G. P. M. van Klink and G. van Koten, *Inorg. Chim. Acta*, 2003, **352**, 247-252; (d) K. Yu, W. Sommer, M. Weck and C. W. Jones, *J. Catal.*, 2004, **226**, 101-110; (e) K. Yu, W. Sommer, J. M. Richardson, M. Weck and C. W. Jones, *Adv. Synth. Catal.*, 2005, **347**, 161-171; (f) D. E. Bergbreiter, P. L. Osburn and J. D. Frels, *Adv. Synth. Catal.*, 2005, **347**, 172-184; (g) M. Akaiwa, T. Kanbara, H. Fukumoto and T. Yamamoto, *J. Organomet. Chem.*, 2005, **690**, 4192-4196; (h) R. Cervantes, S. Castillejos, S. J. Loeb, L. Ortiz-Frade, J. Tiburcio and H. Torrens, *Eur. J. Inorg. Chem.*, 2006, 1076-1083; (i) C. A. Kruithof, H. P. Dijkstra, M. Lutz, A. L. Spek, R. J. M. K. Gebbink and G. van Koten, *Organometallics*, 2008, **27**, 4928-4937.
7. (a) G. Ebeling, M. R. Meneghetti, F. Rominger and J. Dupont, *Organometallics*, 2002, **21**, 3221-3227; (b) C. S. Consorti, G. Ebeling, F. R. Flores, F. Rominger and J. Dupont, *Adv. Synth. Catal.*, 2004, **346**, 617-624; (c) A. Fleckhaus, A. H. Mousa, N. S. Lawal, N. K. Kazemifar and O. F. Wendt, *Organometallics*, 2015, **34**, 1627-1634.
8. (a) Y. Motoyama, K. Shimozone and H. Nishiyama, *Inorg. Chim. Acta*, 2006, **359**, 1725-1730; (b) J.-F. Gong, Y.-H. Zhang, M.-P. Song and C. Xu, *Organometallics*, 2007, **26**, 6487-6492; (c) B. Inés, R. San Martin, F. Churruca, E. Domínguez, M. K. Urtiaga and M. I. Arriortua, *Organometallics*, 2008, **27**, 2833-2839; (d) J. Li, M. Siegler, M. Lutz, A. L. Spek, R. J. M. Klein Gebbink and G. van Koten, *Adv. Synth. Catal.*, 2010, **352**, 2474-2488; (e) B.-S. Zhang, W. Wang, D.-D. Shao, X.-Q. Hao, J.-F. Gong and M.-P. Song, *Organometallics*, 2010, **29**, 2579-2587; (f) J.-L. Niu, Q.-T. Chen, X.-Q. Hao, Q.-X. Zhao, J.-F. Gong and M.-P. Song, *Organometallics*, 2010, **29**, 2148-2156; (g) M.-J. Yang, Y.-J. Liu, J.-F. Gong and M.-P. Song, *Organometallics*, 2011, **30**, 3793-3803; (h) D. E. Herbert and O. V. Ozerov, *Organometallics*, 2011, **30**, 6641-6654; (i) A.-T. Hou, Y.-J. Liu, X.-Q. Hao, J.-F. Gong and M.-P. Song, *J. Organomet. Chem.*, 2011, **696**, 2857-2862.
9. G. R. Fulmer, W. Kaminsky, R. A. Kemp and K. I. Goldberg, *Organometallics*, 2011, **30**, 1627-1636.
10. G. R. Newkome, W. E. Puckett, V. K. Gupta and G. E. Kiefer, *Chem. Rev.*, 1986, **86**, 451-489.
11. For the examples of PCP-H (η^2 -C_{aryl}-H)-M coordination as a key pincer metallation step, see: (a) P. Dani, T. Karlen, R. A. Gossage, W. J. J. Smeets, A. L. Spek and G. van Koten, *J. Am. Chem. Soc.*, 1997, **119**, 11317-11318; (b) A. Vigalok, O. Uzan, L. J. W. Shimon, Y. Ben-David, J. M. L. Martin and D. Milstein, *J. Am. Chem. Soc.*, 1998, **120**, 12539-12544; (c) D. G. Gusev, M. Madott, F. M. Dolgushin, K. A. Lyssenko and M. Y. Antipin, *Organometallics*, 2000, **19**, 1734-1739; (d) J. J. Adams, A. Lau, N. Arulsamy and D. M. Roddick, *Inorg. Chem.*, 2007, **46**, 11328-11334.
12. (a) S. Trofimenko, *Inorg. Chem.*, 1973, **12**, 1215-1221; (b) P. Steenwinkel, R. A. Gossage, T. Maunula, D. M. Grove and G. van Koten, *Chem. Eur. J.*, 1998, **4**, 763-768.
13. (a) P. Steenwinkel, S. L. James, D. M. Grove, H. Kooijman, A. L. Spek and G. van Koten, *Organometallics*, 1997, **16**, 513-515; (b) P. Steenwinkel, R. A. Gossage and G. van Koten, *Chem. Eur. J.*, 1998, **4**, 759-762.
14. S. M. Khake, V. Soni, R. G. Gonnade and B. Punji, *Dalton Trans.*, 2014, **43**, 16084-16096.
15. E. E. Nifant'ev, E. N. Rasadkina, P. V. Slitkov and L. K. Vasyanina, *Phosphorus, Sulfur, and Silicon and Rel. Elem.*, 2003, **178**, 2465-2477.
16. (a) J.-M. Valk, R. van Belzen, J. Boersma, A. L. Spek and G. van Koten, *J. Chem. Soc., Dalton Trans.*, 1994, 2293-2302; (b) J.-M. Valk, J. Boersma and G. van Koten, *J. Organomet. Chem.*, 1994, **483**, 213-216.
17. M. L. Zanini, M. R. Meneghetti, G. Ebeling, P. R. Livotto, F. Rominger and J. Dupont, *Inorg. Chim. Acta* 2003, **350**, 527-536.
18. A. J. Canty, N. J. Minchin, B. W. Skelton and A. H. White, *J. Chem. Soc., Dalton Trans.*, 1987, 1477-1483.
19. (a) S. Pivsa-Art, T. Satoh, Y. Kawamura, M. Miura and M. Nomura, *Bull. Chem. Soc. Jpn.*, 1998, **71**, 467-473; (b) F. Bellina, S. Cauteruccio and R. Rossi, *Eur. J. Org. Chem.*, 2006, 1379-1382; (c) L. Ackermann, A. Althammer and S. Fenner, *Angew. Chem. Int. Ed.*, 2009, **48**, 201-204; (d) F. Shibahara, E. Yamaguchi and T. Murai, *Chem. Commun.*, 2010, **46**, 2471-2473.
20. A. M. van Leusen, B. E. Hoogenboom and H. Siderius, *Tetrahedron Lett.*, 1972, **13**, 2369-2372.
21. A satisfactory elemental analysis is not observed for this compound.
22. APEX2, SAINT and SADABS. Bruker AXS Inc., Madison, Wisconsin, USA. 2006.
23. G. M. Sheldrick, *Acta Crystallogr.*, 2008, **A64**, 112.

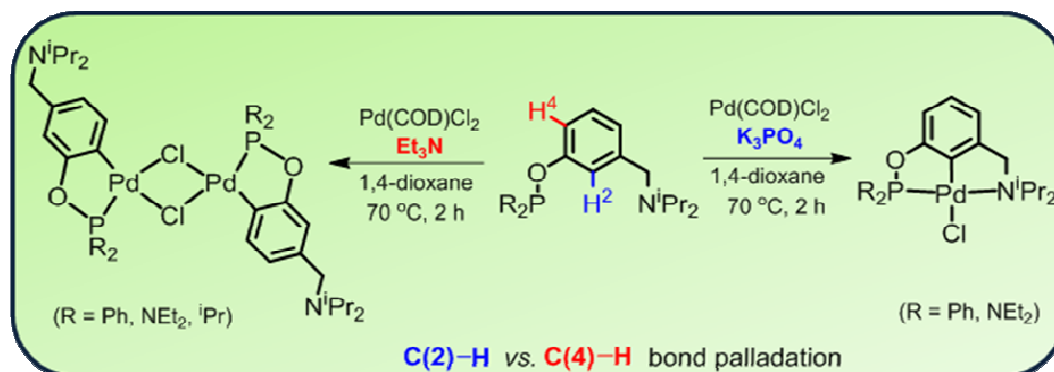
Mono- and binuclear palladacycles via regioselective C–H bond activation: syntheses, mechanistic insights and catalytic activity in direct arylation of azoles

Dilip K. Pandey,^a Shrikant M. Khake,^a Rajesh G. Gonnade^b and Benudhar Punji^{*a}

^a*Organometallic Synthesis and Catalysis Group, Chemical Engineering Division, CSIR–National Chemical Laboratory (CSIR–NCL), Dr. Homi Bhabha Road, Pune – 411 008, Maharashtra, INDIA. Phone: + 91-20-2590 2733, Fax: + 91-20-2590 2621, E-mail: b.punji@ncl.res.in*

^b*Centre for Material Characterization, CSIR–National Chemical Laboratory (CSIR–NCL), Dr. Homi Bhabha Road, Pune – 411 008, Maharashtra, INDIA*

Table of contents entry



Hybrid “POCN”-ligated mono- and binuclear palladacycles have been synthesized *via* the base-assisted regioselective C–H bond activation, and their mechanistic aspects and catalytic application for the arylation of azoles have been described.